

---

# Graph Coloring via Neural Networks for Haplotype Assembly and Viral Quasispecies Reconstruction

---

Hansheng Xue,<sup>1</sup> Vaibhav Rajan,<sup>2</sup> and Yu Lin<sup>1\*</sup>

<sup>1</sup>School of Computing, Australian National University, Canberra, Australia

<sup>2</sup>School of Computing, National University of Singapore, Singapore

{hansheng.xue, yu.lin}@anu.edu.au, vaibhav.rajan@nus.edu.sg

## Abstract

Understanding genetic variation, e.g., through mutations, in organisms is crucial to unravel their effects on the environment and human health. A fundamental characterization can be obtained by solving the haplotype assembly problem, which yields the variation across multiple copies of chromosomes. Variations among fast evolving viruses that lead to different strains (called quasispecies) are also deciphered with similar approaches. In both these cases, high-throughput sequencing technologies that provide oversampled mixtures of large noisy fragments (reads) of genomes, are used to infer constituent components (haplotypes or quasispecies). The problem is harder for polyploid species where there are more than two copies of chromosomes. State-of-the-art neural approaches to solve this NP-hard problem do not adequately model relations among the reads that are important for deconvolving the input signal. We address this problem by developing a new method, called NeurHap, that combines graph representation learning with combinatorial optimization. Our experiments demonstrate substantially better performance of NeurHap in real and synthetic datasets compared to competing approaches.

## 1 Introduction

Our genetic material is organized as sequences of DNA or RNA molecules (nucleotides) which form three-dimensional structures (chromosomes) within our cells. Most organisms have multiple highly similar copies of chromosomes in their cells (e.g., humans have 2). Variations in genetic sequences lead to the emergence of new species during evolution and are also known to be associated with many diseases (e.g., cancer). There are many possible ways in which such variations can occur; the simplest among them is a *mutation* or a change in the nucleotide at a specific location in the DNA or RNA sequence. A Single Nucleotide Polymorphism (SNP) refers to a mutation in at least one of the copies which renders the copies nonidentical at that point. An ordered list of SNPs on a single chromosome is called a haplotype [Schwartz, 2010]. Haplotypes provide a signature of genetic variability and thus inform us about disease susceptibilities and evolutionary patterns (e.g., of viruses). These studies in turn pave the way for personalized medicine and effective drug development against viruses.

The problem of inferring haplotypes from high-throughput sequencing data is called haplotype assembly or phasing, and is done in multiple stages (see Figure 1). Sequencing data yields multiple copies of short fragments of the entire genomic sequence (called reads, Figure 1b). These reads are noisy due to sequencing errors and their short lengths may span across limited number of SNPs. This makes the problem of haplotype phasing challenging. The reads are first aligned to a reference genome. This step indicates positions that are different across reads and thus infers the potential locations of SNPs. All other positions are discarded to obtain the SNP matrix (Figure 1c). This

---

\*Corresponding author.

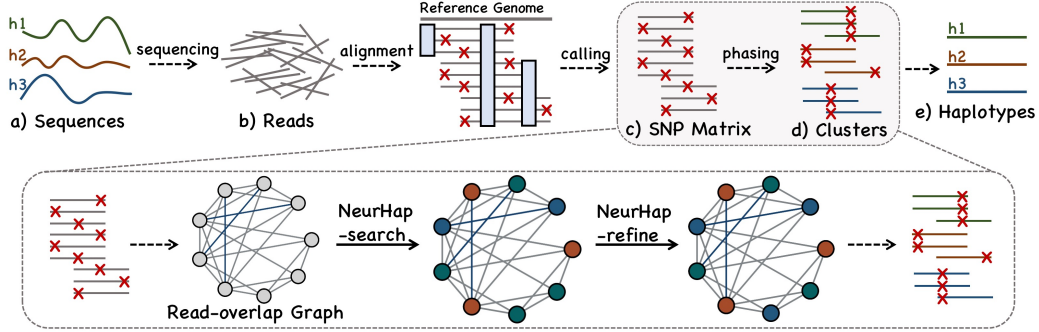


Figure 1: The pipeline of reference-based polyploid haplotypes reconstruction and NeuralHap. Haplotype phasing is formulated as a graph coloring problem by constructing the Read-overlap graph. NeuralHap consists of NeuralHap-search, a graph neural network to learn vertex representations and color assignments, and NeuralHap-refine, a local refinement strategy to further adjust colors.

matrix may be viewed as an oversampled mixture of noisy reads (restricted to SNPs). Each mixture component represents a single haplotype and thus should have SNPs at the same locations.

In diploid species, containing two copies of chromosomes, there are two haplotypes to be inferred. This problem has been studied extensively [Browning and Browning, 2011]. In polyploid species, containing more than two copies of chromosomes (and thus more than two haplotypes), the problem is more challenging due to dramatic increase in search space [Van de Peer et al., 2017, Abou Saada et al., 2022, Jablonski and Beerenwinkel, 2021]. In reconstruction of virus strains, called viral quasispecies, from viral populations, similar challenges arise. Moreover, unknown population sizes and imbalanced abundances pose additional difficulties [Jablonski and Beerenwinkel, 2021].

Existing approaches for haplotype phasing of polyploid species and viral quasispecies often group reads in the SNP matrix into clusters that correspond to different haplotypes, respectively. In an ideal case, all reads from the same cluster should be consistent with respect to SNPs as they all belong to the same haplotype. In reality inconsistencies occur due to sequencing errors in reads. Therefore, a minimum error correction (MEC) score [Lippert et al., 2002b] is used to measure the discrepancy between the consensus haplotypes and their associated reads within each cluster (see Figure 1e). It is NP-hard to optimize the MEC score [Zhang et al., 2006], and a number of combinatorial optimization heuristics have been proposed to approximate the optimal MEC score [Zhang et al., 2020].

More recently, the first neural network-based learning framework, named GAEseq [Ke and Vikalo, 2020b], was proposed to phase haplotypes for polyploid species and viral quasispecies. CAECseq was later developed using a convolutional auto-encoder which captures spatial relationships between SNPs and enables clustering reads obtained from highly similar genomic regions [Ke and Vikalo, 2020a]. Both GAEseq and CAECseq showed improved results compared to previous approaches. A major limitation of both CAECseq and GAEseq is that they cannot capture implicit relations among different reads. These methods have two independent steps (embedding and clustering) which makes the haplotype phasing results unstable. Besides, sparsity of the SNP matrix makes haplotype phasing for polyploids more challenging for these methods as well.

In this paper, we propose an approach based on graph representation learning for haplotype phasing of polyploid species and viral quasispecies. We formulate the haplotype phasing problem as a graph coloring problem, where the colors indicate haplotypes. The graph is constructed from the SNP matrix where vertices are reads and two edge types are defined based on pairwise consistency and conflicts with respect to SNPs in the reads. Message passing-based neural networks are trained to minimize a loss designed to obtain a color assignment that maximizes consistent edges and minimizes conflicting edges. The network learns vertex representations and through them, an initial color assignment. A local refinement strategy is then applied to adjust node colors in order to minimize MEC scores. Thus, in contrast to previous neural approaches that first learn representations and then cluster, our approach models the problem requirements in all steps. As a result, our model achieves better MEC scores, is more stable and also performs well on the challenging cases of polyploids and viral quasispecies. In summary, our contributions are:

- We provide a unique formulation of the haplotype phasing problem as a graph coloring problem, and develop an algorithm based on graph representation learning and combinatorial optimization.
- Our approach consists of NeurHap-search, a graph neural network to learn vertex representations and color assignments followed by NeurHap-refine, a local refinement strategy to adjust colors and optimize MEC scores.
- Extensive experiments on synthetic and real datasets demonstrate that our new method NeuralHap significantly outperforms state-of-the-art phasing methods for both polyploid species and viral quasispecies.

## 2 Related Work

**Haplotype Phasing.** The aim of haplotype phasing of polyploid species and viral quasispecies is to group reads into homogeneous clusters that corresponds to different haplotypes, respectively. The minimum error correction (MEC) score [Lippert et al., 2002b] is introduced to measure the total discrepancy of reads in all clusters but is NP-hard to be optimised [Zhang et al., 2006]. Haplotype phasing for diploid species (i.e., reconstructing two haplotypes) has been extensively studied in the last two decades and a number of combinatorial optimization heuristics have been proposed to approximate the optimal MEC score, such as BNB [Wang et al., 2005], HapCUT [Bansal and Bafna, 2008], HASH [Bansal et al., 2008], RefHap [Duitama et al., 2012] ProbHap [Kuleshov, 2014], HapCUT2 [Edge et al., 2017] and others, and refer to [Zhang et al., 2020] for a recent review on phasing diploid species.

Haplotype phasing for polyploid species (i.e., reconstructing more than two haplotypes) becomes more computationally challenging as it requires a much larger search space compared to phasing two haplotypes for diploid species. A limited number of phasing methods work for polyploid species, e.g., HapCompass [Aguiar and Istrail, 2012], SDhaP [Das and Vikalo, 2015], H-PoP [Xie et al., 2016], AltHap [Hashemi et al., 2018], refer to [Abou Saada et al., 2022] for a recent review. Haplotype phasing for viral quasispecies is very similar to the problem of phasing polyploid species. While haplotypes in polyploid species typically have uniform abundances, the different haplotypes (strains) in viral quasispecies may have varying abundances. Quite a few tools have also been proposed for haplotype phasing of viral quasispecies, such as ViSpA [Astrovskaya et al., 2011], ShoRAH [Zagordi et al., 2011], QuRe [Prosperi and Salemi, 2012], QuasiRecomb [Töpfer et al., 2013], PredictHaplo [Prabhakaran et al., 2014], aBayesQR [Ahn and Vikalo, 2018], TenSQR [Ahn et al., 2018], refer to [Jablonski and Beerenwinkel, 2021] for a recent review.

More recently, deep learning models have been introduced into haplotype phasing for polyploid species and viral quasispecies. GAEseq [Ke and Vikalo, 2020b] uses a graph auto-encoder model on the constructed reads-SNPs bipartite network to model the relations between reads and SNPs. CAECseq [Ke and Vikalo, 2020a] uses a convolutional auto-encoder model to represent reads as low-dimensional features and then employs a clustering algorithm to group these reads. Note that GAEseq and CAECseq can be directly used to phase haplotypes for both polyploid species and viral quasispecies. Experimental results on both simulated and real datasets showed the superior results of GAEseq and CAECseq (in terms of MEC scores) compared to previous approaches for haplotype phasing for both polyploid species and viral quasispecies [Ke and Vikalo, 2020b,a]. However, implicit relations among different reads have not been fully captured by GAEseq and CAECseq, especially when embedding and clustering are modelled separately and the SNP matrix is sparse.

**Neural Networks on Graphs.** Most existing graph neural networks can be explained as a message-passing based graph learning model which recursively combines learned features/messages from their neighbors [Cui et al., 2019, Cai et al., 2018, Gilmer et al., 2017]. Popular methods include GCN [Kipf and Welling, 2017], GraphSAGE [Hamilton et al., 2017], GAT [Veličković et al., 2018] and GIN [Xu et al., 2019]. All these methods make the homophily assumption that similar nodes in the graph should be embedded close together. However, graph coloring aims to assign pairwise nodes with distinct colors for each edge of the graph, which is opposite to the homophily assumption. An intuitive way to integrate GNN models into the graph coloring challenge is to adjust the loss function, such as GNN-GCP [Lemos et al., 2019], RUN-CSP [Toenshoff et al., 2019], and PI-GNN [Schuetz et al., 2022]. However, existing GNN-based graph coloring models cannot be implemented to the read-overlap graph directly because they cannot handle conflicting and consistent edges simultaneously.

### 3 Methodology

**Overview.** In this paper, we propose the model of neural networks for graph coloring optimization to solve the haplotype reconstruction problem, called NeurHap. NeurHap mainly contains three steps, i) constructing the *read-overlap graph*; ii) global coloring searching via iterative neural networks model, NeurHap-search; iii) local refinement to fine tune final coloring, NeurHap-refine.

**Notations.** Let  $k$  be the number of haplotypes in a cell of polyploid species (aka. *ploidy*) or the number of strains in viral quasispecies. For example, human and other mammals contain two haplotypes (diploid,  $k=2$ ); plants have more than 2 haplotypes (e.g., California redwood has six copies of each chromosome, hexaploid,  $k=6$ ). Viral quasispecies mixing 5 distinct HIV strains will have  $k = 5$ .

Single nucleotide polymorphisms (SNPs) refer to positions where not all haplotypes have the same alleles. Given the alignment of reads to a reference genome, the SNP columns can be identified by removing the columns with identical alleles. The remaining alignment is referred to as a  $m \times n$  SNP matrix  $\mathcal{R}$  where  $m$  denotes the number of reads and  $n$  is the number of SNPs. The haplotype reconstruction aims to group  $m$  reads into  $k$  clusters,  $\{C_1, C_2, \dots, C_k\}$ , that correspond to  $k$  haplotypes,  $\{\mathcal{H}_1, \mathcal{H}_2, \dots, \mathcal{H}_k\}$ , respectively. Once reads are grouped into clusters, the haplotype  $\mathcal{H}_i$  can be reconstructed from reads in  $C_i$  using a simple consensus voting. In the ideal case, all the reads from the cluster  $C_i$  will be all consistent with  $\mathcal{H}_i$ . In reality, this is not the case and thus a minimum error correction (MEC) score [Lippert et al., 2002b] is introduced to measure the discrepancy between the reads in the cluster  $C_i$  and the consensus haplotypes  $\mathcal{H}_i$  in all clusters. Given the grouping of reads into  $k$  clusters  $\{C_1, C_2, \dots, C_k\}$ , the corresponding MEC score can be computed as

$$\text{MEC}(C_1, C_2, \dots, C_k) = \sum_{i=1}^k \sum_{R_j \in C_i} HD(\mathcal{H}_i, R_j) \quad (1)$$

where  $HD(\cdot)$  is the Hamming distance function. Note that  $HD(\mathcal{H}_i, R_j)$  for  $R_j \in C_i$  can only be computed when we know all the reads in the cluster  $C_i$  and use them to derive the consensus haplotype  $\mathcal{H}_i$  of  $C_i$ . The main challenge in haplotype phasing is to find the grouping of reads into  $\{C_1, C_2, \dots, C_k\}$  such that the MEC score is minimized.

Two reads are called *overlapping* if they span over common SNP positions otherwise *non-overlapping*. Given any two reads, the relationship between them belongs to one of three cases, *consistent*, *conflict*, or *ambiguous*. While the relationship between two non-overlapping reads is always *ambiguous*, we further introduce two parameters  $p$  and  $q$  to define the relationship between two overlapping reads to account for sequencing errors and alignment ambiguity. Two overlapping reads are *consistent* if they overlap at least  $p$  positions and have the same alleles over all overlapping positions; are in *conflict* if they differ on at least  $q$  overlapping positions; and are *ambiguous* otherwise. The term ‘*ambiguous*’ means that there is not enough evidence to support that these two reads should belong to the same haplotype (‘*consistent*’) or should belong to the different haplotypes (‘*conflict*’). For example, in Figure 2,  $R_4$  and  $R_7$  are *consistent*,  $R_1$  and  $R_2$  are in *conflict*, and  $R_1$  and  $R_4$  are *ambiguous*. In an ideal case, all the overlapping reads in the same cluster must be *consistent*, i.e., if two reads are in *conflict*, they must belong to different clusters. This observation naturally motivates us to build a read-overlap graph to model all reads as vertices and the important pairwise relationships (i.e., *consistent* and *conflict*) between overlapping reads as edges. Moreover, if we use  $k$  colors to represent the  $k$  clusters of reads, the problem of haplotype phasing is reduced to a graph coloring problem on the read-overlap graph. For example, in Figure 2, the minimum MEC is achieved by grouping nine reads into three clusters,  $C_1 = \{R_1, R_4, R_7\}$ ,  $C_2 = \{R_2, R_5, R_8\}$  and  $C_3 = \{R_3, R_6, R_9\}$ , which correspond to three distinct colors on corresponding vertices in the read-overlap graph, respectively.

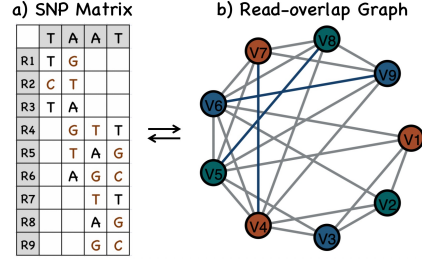


Figure 2: A toy example of constructing *read-overlap graph* with conflict edges (in grey) and consistent edge (in blue).

### 3.1 Graph Coloring over the Read-overlap Graph.

The *read-overlap graph*  $\mathcal{G} = (\mathcal{V}, \mathcal{E}_=, \mathcal{E}_\neq)$  is constructed in this step. Here, the vertex set  $\mathcal{V}$  denotes all reads, the edge set  $\mathcal{E}_=$  represents all pairwise consistent relationships between overlapping reads, and the edge set  $\mathcal{E}_\neq$  refers to the pairwise conflict relationships between overlapping reads.

Now we are ready to reduce the problem of haplotype phasing to the graph coloring problem on the read-overlap graph. Recall that the haplotype phasing problem aims to group reads into  $k$  clusters such that reads from the same cluster are as consistent as possible. If we employ  $c(v)$  to represent one out of  $k$  colors assigned to a read  $v$  (i.e., one of the  $k$  clusters that  $v$  belongs to), two reads  $R_i$  and  $R_j$  are in the same cluster if and only if two corresponding vertices  $v_i$  and  $v_j$  have the same color, i.e.,  $c(v_i) = c(v_j)$ . Now the graph coloring problem needs to assign a color to  $c(v)$  for every vertex  $v \in \mathcal{V}$  to minimise the MEC score under the constraints that any two conflicting reads have two different colors and any two consistent reads have the same color.

$$\begin{aligned} \min \text{MEC}(c(v_1), c(v_2), \dots, c(v_n)) &= \min \sum_{i=1}^k \sum_{c(v_j)=i} \text{HD}(\mathcal{H}_i, R_j) \\ \text{s.t.}, \quad &\begin{cases} \forall (v_i, v_j) \in \mathcal{E}_\neq, c(v_i) \neq c(v_j) \\ \forall (v_i, v_j) \in \mathcal{E}_=, c(v_i) = c(v_j) \end{cases} \end{aligned} \quad (2)$$

Note that the above graph coloring problem is different from the classical graph coloring problem [Pardalos et al., 1998] in combinatorial optimization. While all the edges are conflicting edges in the classical graph coloring problem, the above problem formulation in the equation 2 has constraints for both conflicting and consistent edges. In the following section, we will show how to model these constraints using neural networks.

### 3.2 Network-based Global Search and Combinatorial Optimization-based Local Refinement

**Satisfying Constraints.** As the vertices of the read-overlap graph need to be colored to satisfy the constraints in the equation 2, we further reduce the graph coloring problem to a constraints satisfaction problem inspired by RUN-CSP [Toenshoff et al., 2019]. Graph neural networks (GNNs) are designed to follow homophily constraints such that similar vertices in the graph are embedded close to each other (i.e., same colors). While this is true for consistent constraints in the read-overlap graph, the conflicting constraints impose heterozygous constraints, i.e., vertices connected by a conflicting edge should have very different embeddings (i.e., different colors). Therefore, given  $k$  distinct colors, we introduce two 0/1 metrics in  $\mathbb{R}^{k \times k}$  for incorporating the above two different coloring constraints,  $\mathcal{M}_\neq$  (for conflicting constraints) and  $\mathcal{M}_=$  (for consistent constraints). The conflict-constraint matrix  $\mathcal{M}_\neq$  denotes the binary conflict relationships among  $k$  colors, i.e.,  $\mathcal{M}_\neq(i, j) = 1$  if  $i \neq j$  and 0 otherwise, for any  $i, j \in \{1, \dots, k\}$ . The consistent-constraint matrix  $\mathcal{M}_=$  denotes the consistent relationships between  $k$  colors, i.e.,  $\mathcal{M}_=(i, j) = 1$  if  $i = j$  and 0 otherwise, for any  $i, j \in \{1, \dots, k\}$ .

Assume that the coloring-assignment matrix  $P \in \mathbb{R}^{|\mathcal{V}| \times k}$  is a matrix that represents the coloring assignment probability (over  $k$  colors) for each vertex  $v$  in its corresponding row  $P(v)$ . For any conflicting edge  $(v_i, v_j) \in \mathcal{E}_\neq$  in the read-overlap graph, we aim to assign different colors to  $v_i$  and  $v_j$  and thus maximize the sum of joint-probabilities with different colors, i.e.,  $P(v_i)\mathcal{M}_\neq P(v_j)^\top$ . Symmetrically, for any consistent edge  $(v_i, v_j) \in \mathcal{E}_=$  in the read-overlap graph, we aim to assign the same color to  $v_i$  and  $v_j$  and thus maximize the sum of joint-probabilities with same colors, i.e.,  $P(v_i)\mathcal{M}_= P(v_j)^\top$ . In summary, the unsupervised objective function can be formulated as follows:

$$\mathcal{L} = -\frac{1}{|\mathcal{E}_\neq|} \sum_{(v_i, v_j) \in \mathcal{E}_\neq} \log(P(v_i)\mathcal{M}_\neq P(v_j)^\top) - \lambda \cdot \frac{1}{|\mathcal{E}_|=} \sum_{(v_i, v_j) \in \mathcal{E}_=} \log(P(v_i)\mathcal{M}_= P(v_j)^\top). \quad (3)$$

Here,  $\lambda$  controls the importance of consistent constraints compared to conflicting constraints. We will now show how to use representation learnings to derive a coloring-assignment matrix  $P$  that optimizes the above objective function.

**Global Search: NeurHap-search.** To derive a coloring-assignment matrix  $P$ , we propose to use an iterative message passing-based representation learning model to capture the structural information of the read-overlap graph. The message-passing learning model mainly contains three operation

functions, message-learning, aggregation, and combine operator. Given trainable  $d$ -dimensional embeddings for every nodes  $\{h(v_1), h(v_2), \dots, h(v_n)\}, h(v_i) \in \mathbb{R}^d, v_i \in \mathcal{V}$ , which are initialized by randomly sampling from a uniform distribution, the message passing model can be formulated as:

$$\begin{aligned} h(v_i) &= \text{COMBINE}(m(v_i), h(v_i)), \\ m(v_i) &= \text{AGGREGATE}(\{\text{MESSAGE}(h(v_i), h(v_j)) : v_j \in N(v_i)\}). \end{aligned} \quad (4)$$

Here,  $m(v_i)$  is the learned messages from the neighbors of  $v_i$ , and  $N(v_i)$  is the neighbors of  $v_i$  with respect to conflict edges.  $\text{COMBINE}(\cdot)$  is a combine function and  $\text{AGGREGATE}(\cdot)$  denotes an aggregation function. To search for a simple model, we adopt a recent message updater and mean operator ( $m(v_i) = \frac{1}{|N(v_i)|} \sum_{v_j \in N(v_i)} h(v_j)$ ) as combine and aggregate functions respectively.  $\text{MESSAGE}(\cdot)$  represents the learnable message function, e.g.  $\text{MESSAGE}(h(v_i), h(v_j)) = \text{MLP}(h(v_i) || h(v_j))$ . Two linear layers with activation function (e.g., ReLU) are selected to construct the MLP layer. A simple linear decoder can be used to map the learned node embeddings to the probability of colors:  $P(v_i) = \text{DEC}(h(v_i))$ . The message-passing model is iteratively trained for  $t$  times in each epoch to generate reliable features for each node. The pseudocode for the global search process of NeurHap is as follows:

---

**Algorithm 1:** The Global Search Algorithm NeurHap-search

---

**Data:** SNP matrix  $\mathcal{R}$ ; number of iteration  $t$ ; number of polyploids  $k$ ; dimension of hidden features  $d$ .

**Result:** Assignments  $\mathcal{Y}$ .

```

1  $\mathcal{E}_{\neq}, \mathcal{E}_{=} \leftarrow$  Equation 1 // Construct conflict and consistent edge set
2  $\mathcal{M}_{\neq}(k), \mathcal{M}_{=} (k)$  // Initialize coloring constraints
3  $h \leftarrow \mathbb{R}^d \sim [0, 1)$  // Initialize by a uniform distribution
4 for  $e$  epochs do
5   for  $t$  iterations do
6      $\bar{m}(v_j) = \text{msg}(h(v_i), h(v_j)) = \text{MLP}(h(v_i) || h(v_j))$  // Compute message
7     from  $h(v_i)$  and  $h(v_j)$ 
8      $m(v_i) = \text{agg}(\bar{m}(v_j) : v_j \in N(v_i))$  // Aggregate messages from
9     neighbors of  $v_i$ 
10     $h(v_i) = \text{comb}(m(v_i), h(v_i))$  // Combine messages from  $h(v_i)$  and  $m(v_i)$ 
11  end
12   $P \leftarrow \text{dec}(h(v_i))$  // Compute coloring assignment probs
13   $\mathcal{L} \leftarrow$  Equation 3 // Compute conflict loss
14   $\mathcal{Y} \leftarrow P$  // Compute coloring assignment
15 end

```

---

After optimizing the objective function with NeurHap, we can obtain an initial coloring assignment for vertices that satisfy the constraints in the equation 2 in the read-overlap graph. However, the objective function in equation 2 (i.e., the MEC score) may not be optimized as there may exist multiple coloring assignments that satisfy all constraints. Therefore, we run an additional local refinement step to further optimise the objective function in equation 2.

**Local refinement:** NeurHap-refine. This step mainly searches for possible color adjustments of individual vertices given their associated conflicting and consistent constraints. More specifically, if an individual vertex can be assigned a color different from its current color without violating any of the associated conflicting constraints with the neighboring vertices, the color is changed if a better MEC score is obtained by the change. The refinement algorithm, NeurHap-refine, iteratively explores these possible color adjustments of individual vertices. Refer to Appendix A.1 for the pseudocode.

## 4 Experiments

**Dataset.** To evaluate the proposed method NeurHap, we compare NeurHap with state-of-the-art baselines for both polyploid species and viral quasispecies. i) *Polyploid species:* The Solanum Tuberosum is Tetraploid ( $k=4$ ) and the datasets of Solanum Tuberosum contains both simulated dataset **Sim-Potato** and real-world dataset **Real-Potato**, both downloaded from [Ke and Vikalo, 2020a,b]. **Sim-Potato** contains 40 sub-datasets, which contains ten different samples sequenced at four distinct coverages (5X, 10X, 20X, and 30X). **Real-Potato** is the Chromosome 5 capture-seq

data of a small solanum tuberosum population available at NCBI (accession SRR6173308<sup>2</sup>). Ten samples are generated by randomly selecting ten genomic regions as the reference genome. ii) *Viral Quasispecies*: Three viral quasispecies datasets are downloaded from SAVAGE<sup>3</sup> [Baaijens et al., 2017], including the human immunodeficiency virus (**5-strain HIV**,  $k=5$ ), the hepatitis C virus (**10-strain HCV**,  $k=10$ ), and the zika virus (**15-strain ZIKV**,  $k=15$ ). Ten samples are generated by randomly sampling from each of these three datasets. In this paper, we use BWA-MEM [Li, 2013] to align reads to the reference genome and use the same tool described in CAECseq and GAEseq [Ke and Vikalo, 2020a,b] to derive the SNP matrix from the above alignment to ensure a fair comparison.

**Baseline algorithms.** GAEseq [Ke and Vikalo, 2020b] and CAECseq [Ke and Vikalo, 2020a] are two state-of-the-art approaches that work on both haplotype assembly and viral quasispecies reconstruction. We included two additional methods, H-PoP [Xie et al., 2016], AltHap [Hashemi et al., 2018], that specifically work on haplotype assembly for polyploid species. We also included one additional method, TenSQR [Ahn et al., 2018], that specifically works on viral quasispecies reconstruction. Many other specific methods are not included in this study because GAEseq [Ke and Vikalo, 2020b] and CAECseq [Ke and Vikalo, 2020a] have recently demonstrated their superior performance against other baselines in both haplotype assembly and viral quasispecies reconstruction.

**Experimental setup.** The minimum error correction (MEC) score, given in equation 1, is adopted as the evaluation metric [Lippert et al., 2002a] for both haplotype assembly and viral quasispecies reconstruction. Following the experimental setup in [Ke and Vikalo, 2020a,b], all the algorithms run ten times on each input dataset and the lowest MEC score is reported. The initial number of polyploids  $k$  is known:  $k = 4$  for both Sim-Potato and Real-Potato,  $k = 5$  for 5-strain HIV,  $k = 10$  for 10-strain HCV, and  $k = 15$  for 15-strain ZIKV. The default settings of NeurHap hyperparameter are as follows. The representation dimensions are all empirically set to be 32. The number of iteration  $t$  in NeurHap-search is set to be 10 as default. The parameter  $\lambda$  chooses 0.01 as the default value. The default values for parameters  $p$  and  $q$  are 3 and 5, respectively. The NeurHap model is freely available at <https://github.com/xuehansheng/NeurHap>.

#### 4.1 Performance on Polyploid Species data

Table 1 and 2 show that NeurHap significantly outperforms state-of-the-art baselines, which achieving the lowest MEC scores on both the Sim-Potato and Real-Potato datasets. For Cov-5X of Sim-Potato, the MEC score obtained by NeurHap is 29.9 which is about 3x lower than the lowest scores achieved by baselines (96.2 for CAECseq). For Real-Potato, NeurHap also achieves the lowest MEC scores on all samples. The average MEC score achieved by NeurHap is 371.6 which is significantly lower than the second lowest MEC score obtained by CAECseq, 400. The gap between NeurHap and baselines demonstrates the superiority of our model in polyploid haplotype phasing.

Table 1: Performance comparison on Sim-Potato data.

Model	#Cov 5X	#Cov 10X	#Cov 20X	#Cov 30X
H-PoP	429.0±64.1	933.9±103.6	1782.2±161.8	2826.9±180.7
AltHap	610.9±259.3	722.3±179.1	649.3±369.4	1148.2±509.9
GAEseq	153.7±20.3	261.6±58.7	372.8±74.5	496.9±128.7
CAECseq	96.2±26.9	141.4±40.7	254.2±99.7	372.9±148.9
NeurHap	<b>29.9±5.7</b>	<b>51.9±8.2</b>	<b>92.6±10.6</b>	<b>142.0±23.6</b>

Table 2: Performance comparison on Real-Potato data.

Sample	#1	#2	#3	#4	#5	#6	#7	#8	#9	#10	Avg.
Reads	240	389	274	115	141	398	295	284	489	449	-
SNPs	294	238	83	23	176	198	456	424	236	410	-
H-PoP	705	525	132	4	240	982	981	766	793	1413	654.1±435.6
AltHap	746	572	192	9	299	1295	1021	982	811	1311	723.8±451.1
GAEseq	231	406	97	2	180	873	558	441	592	712	409.2±266.6
CAECseq	229	393	103	1	172	859	522	430	593	698	400.0±260.9
NeurHap	<b>178</b>	<b>343</b>	<b>93</b>	<b>1</b>	<b>163</b>	<b>857</b>	<b>499</b>	<b>384</b>	<b>561</b>	<b>632</b>	<b>371.6±268.9</b>

<sup>2</sup><https://www.ncbi.nlm.nih.gov/sra/SRR6173308>

<sup>3</sup><https://bitbucket.org/jbaaijens/savage-benchmarks>

## 4.2 Performance on Viral Quasispecies data

Table 3 shows the results obtained by NeurHap and baselines for reconstructing viral quasispecies on three datasets respectively, 5-strain HIV, 10-strain HCV, and 15-strain ZIKV. In Table 3, NeurHap significantly outperforms baselines on all 10 samples in these datasets. NeurHap achieves the lowest MEC score in 5-strain HIV (1371.4), which is about 160 lower than the MEC score obtained by CAECseq (1638.5). For 10-strain HCV data, NeurHap also achieves the lowest MEC score 1008.1 and the second lowest MEC score is 1144.3 obtained by TenSQR. With increase in the number of haplotypes (strains), performance of CAECseq and GAEseq deteriorates and while that of NeurHap improves. NeurHap significantly outperforms CAECseq and GAEseq on polyploid haplotypes.

Table 3: Performance comparison on three viral quasispecies datasets.

Dataset		#1	#2	#3	#4	#5	#6	#7	#8	#9	#10	Avg.
5-strain HIV	Reads	967	961	951	961	966	969	962	965	955	971	-
	SNPs	1617	1685	1595	1605	1615	1660	1619	1622	1580	1653	-
	TenSQR	1920	2324	1867	1896	2055	1793	2125	1754	1679	1757	1917.0±198.6
	GAEseq	1981	1953	1678	1806	1905	2007	1819	1746	1702	1747	1834.4±119.6
	CAECseq	<u>1729</u>	<u>1750</u>	<u>1787</u>	<u>1552</u>	<u>1730</u>	<u>1622</u>	<u>1611</u>	<u>1529</u>	<u>1519</u>	<u>1556</u>	<u>1638.5±101.5</u>
NeurHap	<b>1307</b>	<b>1525</b>	<b>1385</b>	<b>1265</b>	<b>1410</b>	<b>1382</b>	<b>1393</b>	<b>1323</b>	<b>1274</b>	<b>1450</b>	<b>1371.4±81.2</b>	
10-strain HCV	Reads	500	498	500	499	498	500	499	500	500	500	-
	SNPs	1770	1712	1794	1749	1741	1759	1786	1765	1743	1808	-
	TenSQR	<u>1081</u>	<u>1037</u>	<u>1106</u>	<u>960</u>	<u>1115</u>	<u>1015</u>	<u>1365</u>	1293	1396	<u>1075</u>	1144.3±151.8
	GAEseq	1270	1121	1301	1171	1245	1152	1371	1105	1152	1200	1208.8±85.8
	CAECseq	1490	1616	1347	1675	1475	1405	1563	<u>1413</u>	<u>1436</u>	1554	1497.4±103.1
NeurHap	<b>1029</b>	<b>990</b>	<b>1097</b>	<b>956</b>	<b>1012</b>	<b>899</b>	<b>1014</b>	<b>1008</b>	<b>1079</b>	<b>997</b>	<b>1008.1±56.3</b>	
15-strain ZIKV	Reads	500	500	500	500	500	499	498	497	499	500	-
	SNPs	2384	2358	2385	2360	2386	2383	2375	2373	2353	2353	-
	TenSQR	<u>941</u>	<u>794</u>	<u>859</u>	<u>869</u>	<u>950</u>	<u>856</u>	<u>848</u>	<u>789</u>	<u>849</u>	<u>758</u>	851.3±61.5
	GAEseq	1470	1585	1515	1590	1713	1363	1523	1348	1618	1393	1511.8±119.4
	CAECseq	2344	2248	2427	2338	2454	2406	2378	2496	2292	2309	2369.2±77.4
NeurHap	<b>718</b>	<b>655</b>	<b>752</b>	<b>721</b>	<b>862</b>	<b>658</b>	<b>694</b>	<b>622</b>	<b>666</b>	<b>675</b>	<b>702.3±67.8</b>	

## 4.3 Visualization

To better understand the phasing results, we use python-iGraph package to visualize the read-overlap graph of Sim-Potato-5X dataset with clustering results from NeurHap, CAECseq, and GAEseq (see Figure 3). Different colors denote distinct haplotypes (the number of haplotypes for Sim-Potato is 4). Grey edges are conflicting edges and blue edges are consistent edges in the read-overlap graph. The color of nodes in Figure 3 are derived from the clusters constructed by different models, i.e., each color indicates a cluster of reads that are inferred to come from the same haplotype. In Figure 3 b) and c), 89 and 133 conflicting edges are violated (i.e., connecting two vertices with the same color) for CAECseq and GAEseq, respectively, while none of the conflicting edges are violated for NeurHap. NeurHap derives a coloring assignment that is most consistent with the conflicting and consistent edges in the read-overlap graph.

Figure 4 shows the search process of NeurHap on the Sim-Potato-5X Sample 1 as an example. The sub-figure a) shows the grid layout of the initial coloring of the read-overlap graph violates significant number of conflicting edges (in grey) and consistent edges (in blue). With the increasing number of epochs, the number of violating constraints (conflicting and consistent edges) decrease significantly.

## 4.4 Experimental Analysis

**Ablation study.** To study the effectiveness of our proposed model, we conduct an ablation study to examine the two algorithmic components in NeurHap, a graph neural network-based algorithm NeurHap-search and a local combinatorial optimisation-based refinement algorithm NeurHap-refine.



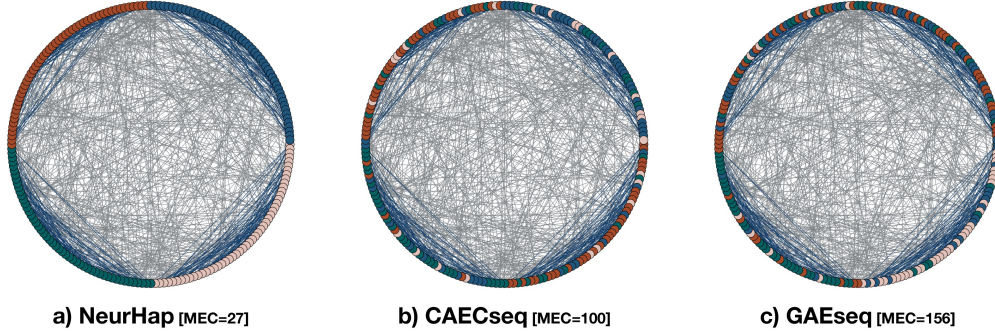


Figure 3: The visualization of NeurHap, CAECseq, and GAEseq on Sim-Potato-5X-Sample1 data.

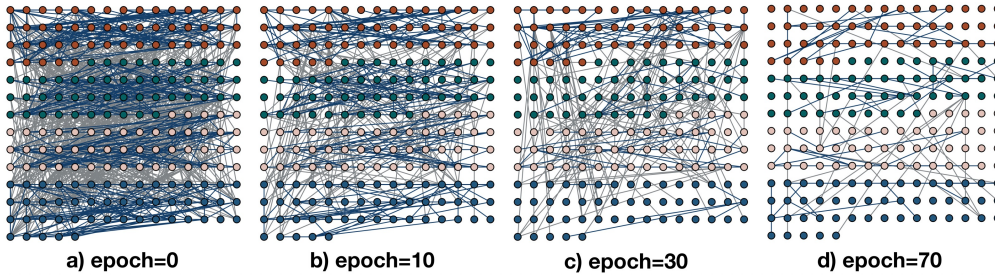


Figure 4: The grid layout of read-overlap graph with the violating edges in the training of NeurHap.

Figure 5 shows that NeurHap-refine is able to further optimize the MEC score, e.g., the MEC scores for 5-strain HIV by NeurHap-search and NeurHap are 1453.5 and 1371.4 respectively, demonstrating the complementary effectiveness of global search and local refinement algorithms on phasing haplotypes.

**Parameter analysis & Running time.** We investigate the importance of core parameters in model, including  $p$  and  $q$  for read-overlap graph,  $\lambda$  for consistent constraints,  $t$  for iterations, and  $d$  for feature dimension. The detailed parameters analysis is listed in the Appendix A.3. We benchmark the running time of NeurHap against two deep learning baselines CAECseq and GAEseq on the Sim-Potato-Cov30 data. NeurHap achieves the lowest MEC score (142.0) compared with CAECseq (372.9) and GAEseq (496.9). The running time of NeurHap is 258 seconds which is faster than CAECseq (341 seconds). GAEseq is the slowest among the three and takes 492 seconds.

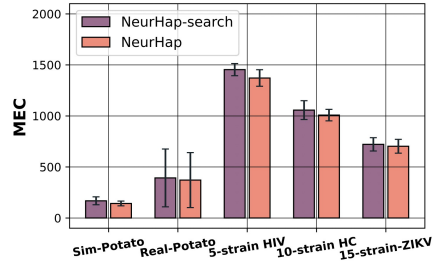


Figure 5: Results of NeurHap-search and NeurHap (NeurHap-search + NeurHap-refine) on all five datasets.

## 5 Conclusion

In this paper, we propose NeurHap, a graph representation learning approach to reconstruct haplotypes of polyploid species and viral quasispecies. We give a novel formulation of the haplotype phasing problem as a graph coloring problem. We design a message-passing based graph neural network search framework over a carefully constructed graph to assign colors (indicating haplotypes) to the reads, and a local refinement step to adjust colors to optimize MEC scores. Extensive experiments on both simulated and real-world datasets demonstrate the effectiveness of our proposed NeurHap model on phasing haplotypes from polyploid species and viral quasispecies. A limitation of our method is in its ability to handle long reads. Massive long reads in polyploids leads to an even larger search space that may be addressed by extensions to our approach in future work. Besides, NeurHap cannot automatically discover the number of haplotypes. This limitation will be addressed going forward.

## References

- Omar Abou Saada, Anne Friedrich, and Joseph Schacherer. Towards accurate, contiguous and complete alignment-based polyploid phasing algorithms. *Genomics*, 114(3):110369, 2022.
- D. Aguiar and Sorin Istrail. Hapcompass: A fast cycle basis algorithm for accurate haplotype assembly of sequence data. *Journal of computational biology*, 19 6:577–90, 2012.
- Soyeon Ahn and Haris Vikalo. abayesqr: A bayesian method for reconstruction of viral populations characterized by low diversity. *Journal of computational biology*, 25:637–648, 2018.
- Soyeon Ahn, Ziqi Ke, and Haris Vikalo. Viral quasispecies reconstruction via tensor factorization with successive read removal. *Bioinformatics*, 34:i23 – i31, 2018.
- Irina Astrovskaya, Bassam Tork, Serghei Mangul, Kelly Westbrooks, Ion I. Măndoiu, Peter Balfe, and Alex Zelikovsky. Inferring viral quasispecies spectra from 454 pyrosequencing reads. *BMC Bioinformatics*, 12:S1 – S1, 2011.
- Jasmijn A. Baaijens, Amal Zine El Aabidine, Eric Rivals, and Alexander Schönhuth. De novo assembly of viral quasispecies using overlap graphs. *Genome research*, 27 5:835–848, 2017.
- Vikas Kumar Bansal and Vineet Bafna. Hapcut: an efficient and accurate algorithm for the haplotype assembly problem. *Bioinformatics*, 24 16:i153–9, 2008.
- Vikas Kumar Bansal, Aaron L. Halpern, Nelson Axelrod, and Vineet Bafna. An mcmc algorithm for haplotype assembly from whole-genome sequence data. *Genome research*, 18 8:1336–46, 2008.
- Daniel Brélaz. New methods to color the vertices of a graph. *Commun. ACM*, 22(4):251–256, 1979.
- Sharon R Browning and Brian L Browning. Haplotype phasing: existing methods and new developments. *Nature Reviews Genetics*, 12(10):703–714, 2011.
- HongYun Cai, Vincent W. Zheng, and Kevin Chen-Chuan Chang. A comprehensive survey of graph embedding: Problems, techniques, and applications. *TKDE*, 30:1616–1637, 2018.
- Peng Cui, Xiao Wang, Jian Pei, and Wenwu Zhu. A survey on network embedding. *TKDE*, 31: 833–852, 2019.
- Shreepriya Das and Haris Vikalo. Sdhap: haplotype assembly for diploids and polyploids via semi-definite programming. *BMC Genomics*, 16, 2015.
- Jorge Duitama, Gayle K McEwen, Thomas Huebsch, Stefanie Palczewski, Sabrina Schulz, Kevin J. Verstrepen, Eun-Kyung Suk, and Margret R. Hoehe. Fosmid-based whole genome haplotyping of a hapmap trio child: evaluation of single individual haplotyping techniques. *Nucleic Acids Research*, 40:2041 – 2053, 2012.
- Peter Edge, Vineet Bafna, and Vikas Kumar Bansal. Hapcut2: robust and accurate haplotype assembly for diverse sequencing technologies. *Genome research*, 27 5:801–812, 2017.
- Justin Gilmer, Samuel S. Schoenholz, Patrick F. Riley, Oriol Vinyals, and George E. Dahl. Neural message passing for quantum chemistry. In *ICML*, 2017.
- William L. Hamilton, Zhitao Ying, and Jure Leskovec. Inductive representation learning on large graphs. In *NeurIPS*, 2017.
- Abolfazl Hashemi, Banghua Zhu, and Haris Vikalo. Sparse tensor decomposition for haplotype assembly of diploids and polyploids. *BMC Genomics*, 19(191), 2018.
- Kim Philipp Jablonski and Niko Beerenwinkel. Computational methods for viral quasispecies assembly. In *Virus Bioinformatics*, pages 51–64. Chapman and Hall/CRC, 2021.
- Ziqi Ke and Haris Vikalo. A convolutional auto-encoder for haplotype assembly and viral quasispecies reconstruction. In *NeurIPS*, 2020a.
- Ziqi Ke and Haris Vikalo. A graph auto-encoder for haplotype assembly and viral quasispecies reconstruction. In *AAAI*, 2020b.

- Thomas N. Kipf and Max Welling. Semi-supervised classification with graph convolutional networks. In *ICLR*, 2017.
- Volodymyr Kuleshov. Probabilistic single-individual haplotyping. *Bioinformatics*, 30:i379 – i385, 2014.
- Henrique Lemos, Marcelo O. R. Prates, Pedro H. C. Avelar, and L. Lamb. Graph colouring meets deep learning: Effective graph neural network models for combinatorial problems. *2019 IEEE 31st International Conference on Tools with Artificial Intelligence (ICTAI)*, pages 879–885, 2019.
- Heng Li. Aligning sequence reads, clone sequences and assembly contigs with bwa-mem. *arXiv: Genomics*, 2013.
- Ross Lippert, Russell Schwartz, Giuseppe Lancia, and Sorin Istrail. Algorithmic strategies for the single nucleotide polymorphism haplotype assembly problem. *Briefings in bioinformatics*, 3(1): 23–31, 2002a.
- Ross Lippert, Russell Schwartz, Giuseppe Lancia, and Sorin Istrail. Algorithmic strategies for the single nucleotide polymorphism haplotype assembly problem. *Briefings in bioinformatics*, 3(1): 23–31, 2002b.
- Panos M Pardalos, Thelma Mavridou, and Jue Xue. The graph coloring problem: A bibliographic survey. In *Handbook of combinatorial optimization*, pages 1077–1141. Springer, 1998.
- Sandhya Prabhakaran, Mélanie Rey, Osvaldo Zagordi, Niko Beerenwinkel, and Volker Roth. Hiv haplotype inference using a propagating dirichlet process mixture model. *IEEE/ACM Transactions on Computational Biology and Bioinformatics*, 11:182–191, 2014.
- Mattia C. F. Prospero and Marco Salemi. Qure: software for viral quasispecies reconstruction from next-generation sequencing data. *Bioinformatics*, 28 1:132–3, 2012.
- Martin J. A. Schuetz, J. Kyle Brubaker, and Helmut G. Katzgraber. Combinatorial optimization with physics-inspired graph neural networks. *ArXiv*, abs/2107.01188, 2022.
- Russell Schwartz. Theory and algorithms for the haplotype assembly problem. *Communications in Information and Systems*, 10(1):23–38, 2010.
- Jan Toenshoff, Martin Ritzert, Hinrikus Wolf, and Martin Grohe. Run-csp: Unsupervised learning of message passing networks for binary constraint satisfaction problems. *ArXiv*, abs/1909.08387, 2019.
- Armin Töpfer, Osvaldo Zagordi, Sandhya Prabhakaran, Volker Roth, Eran Halperin, and Niko Beerenwinkel. Probabilistic inference of viral quasispecies subject to recombination. *Journal of computational biology : a journal of computational molecular cell biology*, 20 2:113–23, 2013.
- Yves Van de Peer, Eshchar Mizrahi, and Kathleen Marchal. The evolutionary significance of polyploidy. *Nature Reviews Genetics*, 18(7):411–424, 2017.
- Petar Veličković, Guillem Cucurull, Arantxa Casanova, Adriana Romero, Pietro Liò, and Yoshua Bengio. Graph Attention Networks. In *ICLR*, 2018.
- Rui-Sheng Wang, Ling-Yun Wu, Zhen-Ping Li, and Xiang-Sun Zhang. Haplotype reconstruction from snp fragments by minimum error correction. *Bioinformatics*, 21 10:2456–62, 2005.
- Minzhu Xie, Qiong Wu, Jianxin Wang, and Tao Jiang. H-PoP and H-PoPG: heuristic partitioning algorithms for single individual haplotyping of polyploids. *Bioinformatics*, 32(24):3735–3744, 2016.
- Keyulu Xu, Weihua Hu, Jure Leskovec, and Stefanie Jegelka. How powerful are graph neural networks? In *ICLR*, 2019.
- Osvaldo Zagordi, Arnab Bhattacharya, Nicholas Eriksson, and Niko Beerenwinkel. Shorah: estimating the genetic diversity of a mixed sample from next-generation sequencing data. *BMC Bioinformatics*, 12:119 – 119, 2011.

Xiang-Sun Zhang, Rui-Sheng Wang, Ling-Yun Wu, and Wei Zhang. Minimum conflict individual haplotyping from snp fragments and related genotype. *Evolutionary Bioinformatics*, 2: 117693430600200032, 2006.

Xingtang Zhang, Ruoxi Wu, Yibin Wang, Jiabin Yu, and Haibao Tang. Unzipping haplotypes in diploid and polyploid genomes. *Computational and structural biotechnology journal*, 18:66–72, 2020.

## A Appendix

### A.1 The pseudocode for NeurHap-refine algorithm

From the previous NeurHap-search step, we obtain an initial coloring assignment for vertices that satisfy the constraints of the read-overlap graph. However, it may exist multiple coloring assignments that satisfy all constraints. Therefore, we run an additional local refinement step to further optimise the MEC score. NeurHap-refine mainly searches for possible color adjustments of individual vertices given their associated conflicting and consistent constraints. More specifically, if an individual vertex can be assigned a color different from its current color without violating any of associated conflicting constraints with the neighboring vertices, the color is changed if a better MEC score is obtained by the change. The local refinement algorithm, NeurHap-refine, iteratively explores these possible color adjustments of individual vertices. The pseudocode for the NeurHap-refine is as follows:

---

**Algorithm 2:** The Local Refinement Algorithm NeurHap-refine.

---

**Data:** Read-overlap graph  $\mathcal{G}$ ; number of polyploids  $k$ ; initial color assignment  $\mathcal{Y}$

**Result:** final color assignments  $\mathcal{Y}^*$ .

---

```

1 Tag ← True // Initialize the iteration tag as True
2 while Tag == True do
3   Tag ← False // Set the iteration tag as False
4   for node  $v \in \mathcal{V}$  do
5      $CN_v \leftarrow \{c(u) \mid (v, u) \in \mathcal{E}_{\neq}\}$  // Compute the set of colors from
        conflicting neighbors
6     for  $c' \notin CN(v)$  and  $c' \neq c(v)$  do
7       // for every possible alternative color  $c'$  for  $v$ 
8        $\mathcal{Y}' \leftarrow \mathcal{Y}_{c(v) \leftarrow c'}$ 
9       //  $\mathcal{Y}'$  is derived by setting  $c'$  as the color of  $v$  in  $\mathcal{Y}$ 
10      if  $MEC(\mathcal{Y}') < MEC(\mathcal{Y})$  then
11         $\mathcal{Y} \leftarrow \mathcal{Y}'$  // Move to a better coloring scheme
12        Tag ← True // Set the iteration tag to be true
13      end
14    end
15  end
16 end
17  $\mathcal{Y}^* \leftarrow \mathcal{Y}$  // Output the final coloring scheme

```

---

### A.2 Implementation Details

Two categories of datasets are used in the paper, *Polyploid species* and *Viral Quasispecies*. *Polyploid species* contains two datasets, Sim-Potato ( $k = 4$ ) and Real-Potato ( $k = 4$ ), which are downloaded from CAECseq [Ke and Vikalo, 2020a] and GAExeq [Ke and Vikalo, 2020b]. *Viral Quasispecies* contains three datasets, 5-strain HIV ( $k = 5$ ), 10-strain HCV ( $k = 10$ ), and 15-strain ZIKV ( $k = 15$ ), which are downloaded from SAVAGE [Baaijens et al., 2017]. It has two steps to generate the SNP matrix, i) Align reads to a reference genome and ii) Extract the matrix from the alignment.

**i) Align Reads to Reference.** BWA-MEM [Li, 2013] is used to align reads to the reference genome. The detailed command is (take the 15-strain ZIKV as an example):

```

$ ./bwa index 15-strain-ZIKV.fasta
$ ./bwa mem 15-strain-ZIKV.fasta forward.fastq reverse.fastq >
15-strain-ZIKV.sam

```

**ii) Extract the SNP Matrix.** We use the same tool described in CAECseq and GAEseq [Ke and Vikalo, 2020a,b] to derive the SNP matrix from the above alignment to ensure a fair comparison. The default parameters are used in the configure file which is same with CAECseq and GAEseq. The detailed command is:

```
$ ./ExtractMatrix config
```

For all five datasets, we randomly generate 10 samples. The detailed number of reads and SNPs for Real-Potato, 5-strain HIV, 10-strain HCV, and 15-strain ZIKV are listed in the paper. For Semi-Potato, sequencing coverage is varied from 5X to 30X. We have 40 sub-datasets in Semi-Potato. The read numbers range from approximately 200 to 1200 and the number of SNPs vary from 200 to 400.

**Read-overlap Graph.** After obtaining the SNP matrix, we build the consistent and conflicting edges between pairs of reads (i.e., pairs of rows in the SNP matrix). Two parameters are introduced in this step to the construct read-overlap graph,  $p$  and  $q$ . Two overlapping reads  $R_i$  and  $R_j$  are *consistent* if they have the same alleles over all SNP positions meanwhile the length of overlapping is larger than  $p$  (i.e.,  $HD(R_i, R_j) = 0$ ), and are in *conflict* if they differ on at least  $q$  SNP positions (i.e.,  $HD(R_i, R_j) \geq q$ ), where  $HD(R_i, R_j)$  represents the Hamming distance between two overlapping reads in the read-overlap graph. We adjust two thresholds according different datasets from 2 to 6, and we also evaluate the effect of two parameters for the NeurHap model.

You can simply run the following to reproduce the experimental results (we take the Sim-Potato-Cov5 Sample 1 as an example).

```
$ python main.py -e 2000 -t 10 -f 32 -k 4 -r 1e-3 -p 6 -q 2 -l 0.01 -d
Semi-Potato -s Sample1
```

where parameter  $-e$  represents the number of epoch,  $-t$  is the number of the iteration,  $-f$  is the dimension of the embedding,  $-k$  is the number of haplotypes or ploids,  $-r$  is the learning rate,  $-l$  denotes the  $\lambda$ . Parameters  $-d$  and  $-s$  are used to select the corresponding data and sample. The source code of NeurHap is freely available at <https://github.com/xuehansheng/NeurHap>.

**Running environment.** NeurHap is implemented in Python 3.6 and Pytorch 1.8 using the Linux server with 6 Intel(R) Core(TM) i7-7800X CPU @ 3.50 GHz, 96GB RAM and 2 NVIDIA RTX A6000 with 48GB memory.

### A.3 Experimental Analysis

**Parameters Analysis.** In this section, we investigate the importance of core parameters in model, including  $p$  and  $q$  for read-overlap graph,  $\lambda$  for consistent constraints,  $t$  for iterations, and  $d$  for feature dimension. Figure 6 b) shows that our proposed NeurHap is robust to the dimension of latent embedding  $d$ . In Figure 6 a), the MEC scores for NeurHap with  $\lambda$  varying from 0.0 to 0.1 do not change too much and relatively stable. However, if we choose  $\lambda$  as 0.5, the performance of NeurHap being worse. We vary  $\lambda$  from 0.0 to 0.1 for NeurHap.

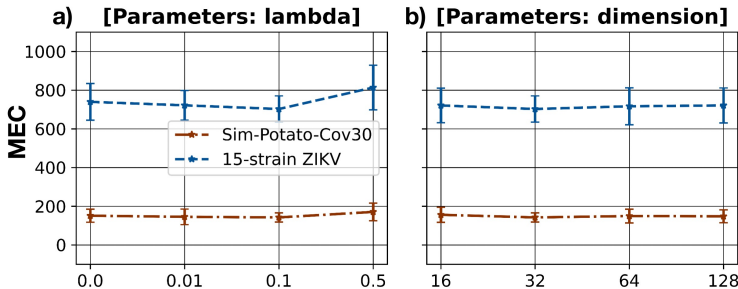


Figure 6: Parameters analysis of the NeurHap model ( $\lambda$  and  $d$ ).

Next, we investigate the effects of parameters  $t$ ,  $p$ , and  $q$  (take the Sim-Potato-Cov30X Sample 1 as an example). We vary iteration  $t$  from 5 to 25 and the results are shown in Figure 7 a). When the iteration  $t = 10$ , NeurHap achieves the best performance on the Sim-Potato-Cov30X Sample 1 dataset. When the iteration  $t \geq 10$ , the MEC score of the NeurHap is relatively stable. In Figure 7 b), When parameters  $q = 4$  and  $p = 5$ , the NeurHap achieves the best performance. If the parameter

$p < 5$  ( $q$  is fixed to 4), the MEC score of the NeurHap is high because the constructed consistent edges are not confident and they contain several mistaken consistent edges. When the parameter  $q > 4$  (the  $p$  is fixed to 5), the number of extracted conflicting edges is few (the read-overlap graph is sparse) which is not good to optimise the MEC score.

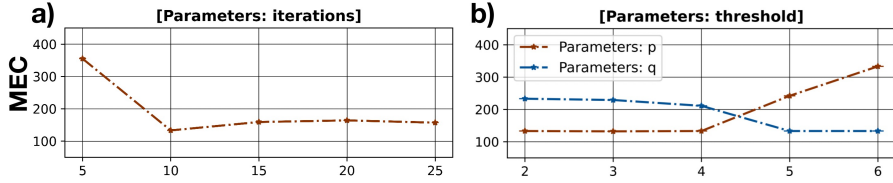


Figure 7: Parameters analysis of the NeurHap model ( $t$ ,  $p$ , and  $q$ ).

**Running Time.** We benchmark the running time of NeurHap against two deep learning baselines CAECseq and GAEseq on the Sim-Potato-Cov30 Sample 1 data. NeurHap achieves the lowest MEC score (142.0) compared with CAECseq (372.9) and GAEseq (496.9). The running time of NeurHap is 258 seconds which is faster than CAECseq (341 seconds). GAEseq is the slowest among the three and takes 492 seconds.

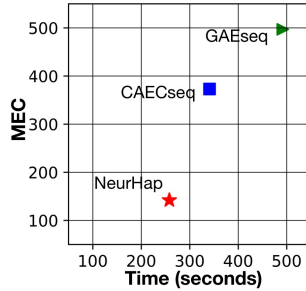


Figure 8: The running time of NeurHap, CAECseq and GAEseq.

#### A.4 Additional Experiment

**Average MEC on Semi-Potato.** In the experimental part, we select the lowest MEC score as the final results after running experiment 10 times which is same as previous SOTA baselines Ke and Vikalo [2020a,b]. Here, we also report the average MEC score after running all algorithms on Semi-Potato 10 times (see Table 4). NeurHap still outperforms other SOTA baselines.

Table 4: Performance comparison on Sim-Potato (Tetraploid,  $k = 4$ ).

Polyploids	Model	#Cov 5X	#Cov 10X	#Cov 20X	#Cov 30X
Tetraploid ( $k=4$ )	H-PoP	429.0±64.1	933.9±103.6	1782.2±161.8	2826.9±180.7
	AltHap	610.9±259.3	722.3±179.1	649.3±369.4	1148.2±509.9
	GAEseq	225.1±17.7	391.2±45.5	610.4±97.3	811.8±131.8
	CAECseq	160.5±25.9	266.0±43.3	466.5±89.0	629.5±160.0
	NeurHap	<b>37.5±5.5</b>	<b>62.8±7.5</b>	<b>113.2±19.8</b>	<b>166.3±26.7</b>

**Benchmark against Graph Coloring.** We also benchmark NeurHap against two graph coloring algorithms, including Greedy [Brélaz, 1979] and RUN-CSP [Toenshoff et al., 2019]. We implement graph coloring algorithms on the read-overlap graphs which only contain conflicting edges because those methods cannot address the consistent edges. In Table 5, NeurHap significantly outperforms graph coloring algorithms.

**MEC score v.s. Violating Constraints.** While Eqn. 2 aims to minimize the sum of hamming distances between each read  $\mathcal{R}_j$  and the haplotype  $\mathcal{H}_i$  that is drawn from  $\mathcal{R}_j$ , Eqn. 3 aims to minimize the divergence between pairs of reads (as  $P(v_i)$  and  $P(v_j)$ ) that are drawn from the same



Table 5: Performance comparison on Real-Potato ( $k = 4$ ) and 5-strain HIV ( $k = 5$ ).

Data	Model	# 1	# 2	# 3	# 4	# 5	# 6	# 7	# 8	# 9	# 10	# Avg.
Real-Potato	Greedy	296	458	162	3	239	1014	679	602	694	906	505.3±330.3
	RUN-CSP	186	358	107	1	185	890	553	492	647	767	418.6±298.7
	NeurHap	<b>178</b>	<b>343</b>	<b>93</b>	<b>1</b>	<b>163</b>	<b>857</b>	<b>499</b>	<b>384</b>	<b>561</b>	<b>632</b>	<b>371.6±268.9</b>
5-strain HIV	Greedy	3974	3791	3633	3819	4251	3472	3137	3241	3326	3476	3612.0±349.3
	RUN-CSP	2226	2375	2175	2408	2192	2748	2449	2614	2312	2567	2406.6±191.3
	NeurHap	<b>1307</b>	<b>1525</b>	<b>1385</b>	<b>1265</b>	<b>1410</b>	<b>1382</b>	<b>1393</b>	<b>1323</b>	<b>1274</b>	<b>1450</b>	<b>1371.4±81.2</b>

haplotype and maximize the divergence between pairs of reads if they are drawn from different haplotypes. Moreover, the hamming distances in Eqn.2 have been used implicitly to derive in Eqn.3. In an ideal case, if all pairs of conflicting reads are assigned into different haplotypes (i.e., different colors) and all pairs of consistent reads are assigned into the same haplotypes (i.e., the same color), each cluster will only contain consistent reads and thus the MEC score in Eqn.2 will be minimized to be 0. In non-ideal cases such as Sim-Potato Cov-5X Sample 1 datasets, the following Figure 9 shows that the objective function to be minimized in Eqn.2 (i.e., MEC) correlates well with the objective function to be minimized in Eqn.3, which demonstrates the effectiveness of NeurHap for minimizing the MEC through optimizing Eqn.3.

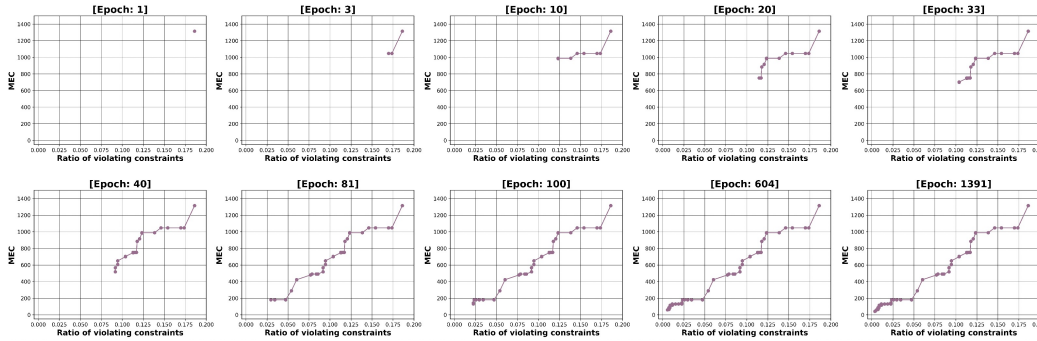


Figure 9: The MEC score v.s. Violating Constraints in the training process of NeurHap.

**Scalability.** To evaluate the scalability of the NeurHap, we incrementally combine the samples in Real-Potato dataset and summarise the results in Table 6. It is observed that the running time of NeurHap is roughly linearly correlated with the number of total edges (conflict edges + consistent edges). On the other hand, diploid haplotype assembly remains challenging for reconstructing chromosome-level haplotypes, especially for large eukaryotic genomes with complex repeats. Similar to CAECseq and GAECseq, NeurHap has also focused on short-read datasets on gene regions because complex repeats in the intergenic regions along the chromosome make it impossible to reconstruct continuous haplotypes reliably.

Table 6: Performance comparison on cumulative Real-Potato dataset.

Samples		# 1	# 2	# 3	# 4	# 5	# 6	# 7	# 8	# 9	# 10
Reads		240	629	903	1018	1159	1557	1852	2136	2625	3074
	SNPs	295	533	616	639	815	1013	1469	1893	2129	2539
	Conflict	3351	6380	13433	14208	16207	34288	39368	42811	51358	59621
	Consistent	966	1514	3323	3537	3908	5747	6470	6977	7985	9329
CAECseq	MEC	229	786	910	985	1282	1997	2584	3018	3914	4524
	time	243s	283s	302s	310s	414s	586s	798s	1188s	1991s	2774s
NeurHap -search	MEC	183	559	671	692	888	1802	2305	2667	3316	3992
	time	28s	38s	52s	53s	63s	99s	128s	157s	200s	253s

Besides, we applied NeurHap on a chromosome-level dataset for Chromosome 22 of the human genome to validate the scalability of NeurHap. Specifically, we downloaded publicly

available alignment files for the Human Genome NA12878 (from <http://s3.amazonaws.com/nanopore-human-wgs/NA12878-Albacore2.1.sorted.bam>) and combined them with the set of heterozygous SNPs on Chromosome 22 of the human genome (derived from [Duitama et al., 2012]) to build the input alignment matrix (following the same procedure introduced in HapCUT2 [Edge et al., 2017]). This constructed matrix contains 129,338 long reads and 22,792 SNPs. NeurHap took 734 seconds and around 13G memory to reconstruct two chromosome-level haplotypes with a MEC score of 23,114. As Chromosome 22 is about 1.6% of the whole human genome and 20% of the largest chromosome (Chromosome 1) in the human genome, we estimate (optimistically) that phasing all the chromosomes in the human genome will take about 12 hours with a peak memory of 65G. Note that CAECseq and GAEseq are both out of the memory when they were applied to this chromosome-level dataset on the NVIDIA RTX A6000 with 48GB memory.